Journal Title
XX(X):1–11

DOI: 10.1177/ToBeAssigned
www.sagepub.com/
SAGE

Computationally efficient modeling of load dynamics in turbocharged internal combustion engines

Mika Laurén[1], Giota Goswami[2], Tuomo Lindh[3] and Jussi Sopanen[2]

Abstract

Hybridization of non-road mobile machinery offers benefits for energy efficiency and decarbonization tasks. Hybrid electric power trains combine combustion engines with electric machines and batteries. Thus, it is important to model engine dynamics accurately so that the operation of different kinds of power train systems can be controlled and optimized. This study compares several transfer function- and time-series-based methods to model dynamic torque in combustion engines. Models are compared with experimental data on real engines. A new simulation method called Dynamic Torque Limiter (DTL) is developed and validated. The DTL method employs both a time-based limitation parameter, which models the turbocharger lag, and a transfer function, which models the fuel injection dynamics of the typical engine.

Keywords

Internal combustion engine, modeling, power train development, non-road mobile machinery, dynamic torque

Introduction

Hybrid power trains, which combine electric drives powered by an internal combustion engine (ICE) and a battery, form a logical pathway to the transition from traditional ICE-based power trains to fully electric ones. Such power trains can reduce emissions and improve efficiency while still benefiting from the existing infrastructure and refueling options available for internal combustion engines. The dimensioning and operation of hybrid electric non-road mobile machinery (NRMM) are presented in several studies for various applications, such as loaders and excavators (1), agricultural tractors (2; 3) and mining loaders (4).

The behavior of the ICE plays an important role in hybrid electric power trains. Comprehensive physical modeling of the ICE is very complex, especially when considering the modeling of engine dynamics. Thus, computationally efficient ICE models are typically based on steady-state measurements on engine test benches. While the load changes of NRMM are highly dynamic, the dynamic response capability of ICEs has certain limitations, especially in turbocharged engines. The dynamics of the load response phenomena of the ICE are divided into gas dynamics, turbocharger lag effects, fuel injection limitations, and thermal delays. They are presented, for instance, by (5). Gas and fuel injection dynamics are typically very fast, and their modeling requires a complex model of the intake and exhaust system. Turbocharger delay is typically measured in a couple of seconds, and it has a significant effect on the engine output especially when the torque demand is increasing. Engine thermal inertia is important in high-level load changes, and it can last tens of seconds or several minutes when the engine has reached a steady condition. This study focuses on the modeling of turbocharger lag, whereas the other effects are not considered.

Matching the turbocharger to the engine typically requires a compromise between the low-speed transient response and the high-speed power output (6). To minimize this compromise and improve the load response capacity of engines, different turbocharging technologies, for example, variable geometry turbine (VGT) and series-charging systems, were presented in (7). Electric-assisted turbochargers are also the focus of several articles (8), (9), (10). These methods have significantly improved the turbocharging performance over the last decades; nevertheless, the performance is limited in some applications. One example of this is the load response of diesel–electric gensets. The electricity-producing quality classes of a diesel genset in a transient situation are defined in (11). This classification is based on the brake mean effective pressure (p_e) of the ICE. At a higher level of p_e, the power production of the ICE is related to the more turbocharged air flow; therefore, the power production capacity of the ICE is limited during sudden load increases. Modeling methods of electric-assisted gensets are presented in (12), while in (13) the focus is on dynamic modeling and exhaust gas emission prediction methods of genset systems.

The modeling of the thermal inertia of ICE components, energy transfer, and turbocharger delays is addressed in (14). The use of emission reduction techniques, such as

[1]Department of Mechanical Engineering, Turku University of Applied Sciences, 20520 Turku, Finland
[2]Department of Mechanical Engineering, Lappeenranta–Lahti University of Technology (LUT), 53850 Lappeenranta, Finland
[3]Department of Electrical Engineering, Lappeenranta–Lahti University of Technology (LUT), 53850 Lappeenranta, Finland

Corresponding author:
Mika Laurén, Department of Mechanical Engineering, Turku University of Applied Sciences, 20520 Turku, Finland.
Email: mika.lauren@turkuamk.fi

exhaust gas recirculation (EGR), has significant effects on the dynamic behavior of the ICE. References (15) and (16) studied the simulation of the control system of the EGR. Paper (17) focused on the EGR- and VGT-equipped engine flow simulation of intake and exhaust manifolds. These ICE systems were modeled as single-volume-based, constant-efficiency basic thermodynamic models.

Eriksson (18) presented a zero-dimensional turbocharger model with surge capability, including several simplified approaches in the model. In these approaches, the turbine efficiency model was based on the blade speed ratio, and black box models were implemented for the mass flow properties of the turbochargers. Surge simulation with two parallel-connected turbochargers is presented in (19), where a Moore-Greitzer-based compressor model employs speed and mass flow maps of a compressor. Black box-type time series models and machine learning-based methods have been developed in several papers, for instance, (20), (21), and (22) for the engine response modeling. In the reference (23) focused on the dynamic exhaust gas emission modeling principle based on the Volterra time series method. Their method was implemented to predict the exhaust gas emission and temperature of the passenger car diesel engine in the New European Driving Cycle.

Various ICE dynamic models were compared by (24), including an analytical model, a nonlinear dynamic model, and a transfer-function-based model. Galindo et al. (25) showed an application of an artificial neural network to predict the Wiebe combustion parameters in in-cylinder combustion. The reference (26) presented construction of an automatized transfer function model of a diesel engine with various constant break torques at a constant torque in a power increase test. The approach is based on the method of moments, where the impulse response of the system is identified and the parameters are automatically determined. For simplified modeling of the transient behavior of turbocharged engines, The reference (6) proposed a second-order TF model instead of more complex models. All these dynamic models reviewed for the present study indicate that accurate modeling of the ICE dynamics requires a large set of data or highly accurate experimental data of engine components. Therefore, the present work continues from a previous study, in which the fuel consumption of the combustion engine was predicted using data provided by the manufacturer (27). The previously presented method did not consider the dynamic response of the engine. However, in the modeling and optimization of hybrid electric power trains, it is important to take account of the realistic dynamic behavior of the ICE.

This paper presents a computationally efficient method for modeling the dynamic torque behavior of an ICE for hybrid electric power train studies. A Dynamic Torque Limiter (DTL) model is proposed and compared with TF- and linear time-series-based models by using real engine data. The proposed modeling method combines the TF-based model and the time-based torque limiter parameter. This limiter parameter can predict the realistic behavior of turbocharger lag for a sudden load increase and the TF parameter for modeling decreasing torque ramps. In addition, the limitation parameter can be connected to the engine speed, enabling modeling of the natural behavior of the turbocharger lag at different engine speeds. The proposed calculation method has only a few parameters to calibrate, which allows it to be easily fitted to real engine data.

Load response modeling methods

This section presents different modeling methods of engine load responses. TF models with different orders, two different parallel TFs (2TF), and an autoregressive time series model with moving average (ARMAX) and without (ARX) are presented. To address the shortcomings of these methods, a new Dynamic Torque Limiter (DTL) model is proposed.

Phenomenon of the load response delay of a charged engine

Typically, the dynamic load response of a turbocharged diesel engine is limited. The smoke and particulate emissions of the diesel engine start to increase strongly when there is not enough combustion air during a sudden increase in the load (13). Therefore, the fuel injection system limits the quantity of fuel to avoid particulate emissions. As a result, the exhaust energy is limited during the load step, and turbocharger operation is further delayed. The turbocharger delay is the main reason behind any insufficient engine load response. It is, therefore, crucial to fit together the turbocharger and the engine to improve the engine load response capability, even though the delay cannot be completely avoided in high-power engines (5).

There is a relation between the load response capability, the engine torque, and the amount of charged air. Below the torque level of a naturally aspirated engine, the engine reacts quickly to torque changes because the combustion air flow is sufficient without charging. According to (28), a naturally aspirated four-stroke diesel engine can produce approximately 0.8–0.9 MPa of brake mean effective pressure (p_e) at the full load. If the torque and thereby the amount of engine air induction are increased by turbocharging above the naturally aspirated level, the torque delay increases. This occurs because the turbocharger is powered by the energy from exhaust gases, which depends on the amount of fuel fed to the engine. On the other hand, the increase in fuel is also limited owing to the lack of combustion air, which, in turn, limits the torque rate. Currently, turbocharged diesel engines can achieve p_e values of 2.5–2.7 MPa with a single turbocharger and even higher values with a series-charged system (5). Thus, the load response capability is typically lower in high-power output engines than in low-power output engines.

One transfer function and two parallel transfer functions

Transfer functions (TF) are mathematical descriptions widely used in control system modeling and electronics. A TF depicts the dynamic output of a linear system in the frequency domain when the input signal is known. The degree of a TF describes the number of zeros and poles of the system. In this study, for the sake of simplicity, low-order TFs were chosen. Six TFs of different orders were fitted separately to real engine load steps at different engine

speeds. The fitted data were assessed using squared residual (R^2) values between the real output torque of the engine and the modeled output torque.

Tupitsina et al. (1) proposed two first-order (1 pole, 0 zeros) TFs for dynamic torque modeling, which were connected in parallel in the torque input. A schematic of this 2TF method is presented in Figure 1. Through the minimizing function, a different dynamical behavior can be chosen for increasing and decreasing torque ramps. A slower response is implemented as a gaseous dynamic response in an increasing ramp, and a faster response is implemented as a fuel-governed response in a decreasing ramp. A benefit of this method is that the delay parameter can be easily attached to the engine speed to maintain the slow reaction of the turbocharger at lower engine speeds. On the other hand, a disadvantage of this method is its discontinuity, meaning that it is not possible to reconstruct the parameters backward by analytical methods from the output results.

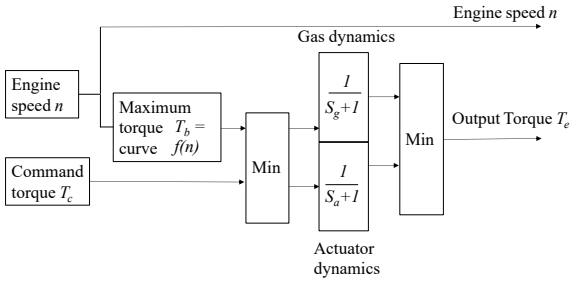

Figure 1. Principle of two parallel first-order transfer functions (2TF) according to (1).

Autoregressive time series

Time series models predict the trends and sequences of the past data. Time series can be obtained by using several methods, such as basic moving average-type calculations and complex nonlinear methods, depending on the prediction requirements. This study focuses on two statistical models: an autoregressive model with an exogenous input (ARX) and an autoregressive model with a moving average and an exogenous input (ARMAX). These models use autoregression, differencing, and moving average methods. Additionally, the models incorporate an exogenous input, to which the commanded torque is connected. The ARX method is described in Equation (1), and the ARMAX method can be described using Equation (2), respectively (29)

$$A(q)y(t) = \sum_{i=1}^{nu} B_i(q)u_i(t - n_{k_i}) + e(t) \quad (1)$$

$$A(q)y(t) = \sum_{i=1}^{nu} B_i(q)u_i(t - n_{k_i}) + C(q)e(t) \quad (2)$$

where A, B, and C are polynomial coefficients presented as functions of the time-shift operator q. The input and output of the model are $u(t)$ and $y(t)$, respectively. n_{k_i} is the time delay of the input signal, and $e(t)$ is the white noise.

Dynamic Torque Limiter (DTL) Method

There are two main disadvantages of the TF and time series models. The first is the limited accuracy of the adjustment of both increasing and decreasing torques, and the other is the unsatisfactory fitting of the increase in the torque step of a charged engine. By using two different parallel TFs (the 2TF method), the fitting results of increasing and decreasing steps can be significantly improved. The proposed Dynamic Torque Limiter method (DTL) is based on one TF in addition to a time-based limiter parameter, which can model the delay of a turbocharger and its effect on torque. The operating principle of the turbocharger affects the torque at higher torque values. To model this behavior, two torque curves are formulated—a naturally aspirated maximum torque curve (NAC) and a boosted torque curve (BOC). The NAC is a virtual curve and exists only computationally. The accurate NAC torque (T_n) at each engine speed is unknown. However, the curve can be constructed such that at the lowest and at the rated engine speeds, the p_e values are set to 0.8 MPa. A p_e value of 0.9 MPa is used at the speed at which the maximum torque occurs. These points can be fitted on a polynomial curve or linearly interpolated so that all p_e values can be calculated.

The BOC curve (T_b) is the real engine maximum torque curve as a function of engine speed, and it limits the model output torque in all conditions. The calculation principle of the DTL method is presented in Figure 2. The instant commanded torque (T_c) is compared with the NAC (T_n) and BOC (T_b) torques. When T_c is below T_n, the TF-based delay parameter (S_d) limits the output. When T_c is higher than the naturally aspirated torque level T_n of the engine, the DTL parameter (T_d) limits the torque increase rate to model the turbocharger delay. A minimizing function selects the lowest instantaneous torque, and in addition, the delay parameter (S_d) simulates the delay in the whole system response. It must be noted that the dynamic torque limitation (DTL) parameter (T_d) is a time-based (Nm/s) limiter, which can be a constant value or a function, for example, of engine speed. Within this study, the DTL parameter is modeled as a first-order function of the engine speed as follows

$$T_d = an + b \quad (3)$$

where a and b are calibration parameters, and n is the engine speed. The parameters a and b can be calibrated using existing engine data. Due to the principle of the DTL method, one disadvantage is its discontinuity. Thus, the input–output results cannot be used afterward for the parameter approximation.

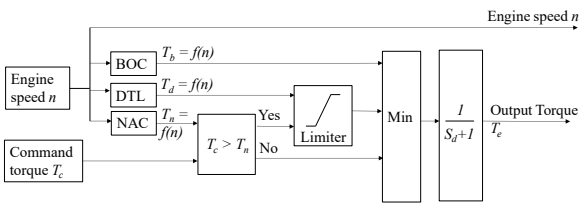

Figure 2. Principle of the DTL method.

Fitting and validation of the different models by using real engine data

The static and dynamic performance of a typical NRMM diesel engine was measured in the engine laboratory of Turku University of Applied Sciences, Finland. The engine had four cylinders, it was single-stage turbocharged, and it was connected to an eddy current dynamometer for torque measurement. The dynamometer inertia was eliminated computationally from the measured torque results so that the dynamic torque in the engine flywheel would be visible in the presented results. The engine and dynamometer test setup is shown in Figure 3, and its specifications are given in Table 1.

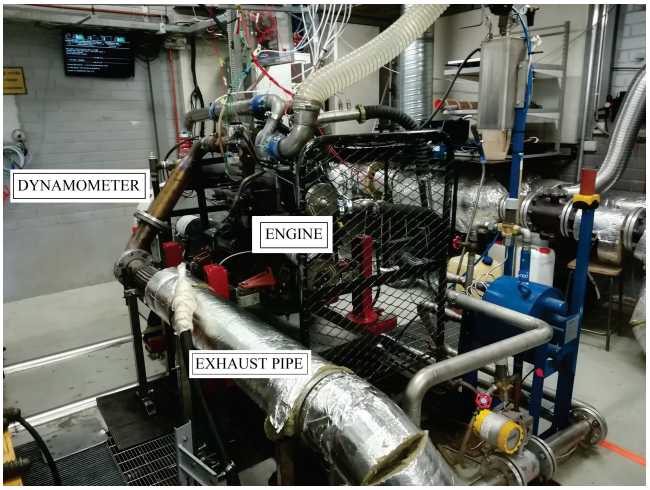

Figure 3. Experimental setup of the research engine.

Table 1. Test setup specifications of the experimental engine .

Type	4 cylinder, 4 stroke diesel
Charging	1-stage turbocharger
Charge adjusting	Electronically controlled waste gate
Charge cooling	Air-to-water cooler
Maximum power	148 kW @ 1950 rpm
Bore and stroke	108 mm and 134 mm
Compression ratio	17.4
Fuel injection	Common-Rail system
Dynamometer	Horiba WT-300
Controller	Horiba SPARK and Labview

Model fitting

A highly dynamic test cycle was used in the laboratory experiments. The engine started to operate at a low torque and speed. Thereafter, the torque was suddenly increased to the maximum value. This procedure was repeated at six different engine speeds. When the commanded torque (T_c) values were increased to the maximum possible level, the engine speed was also simultaneously increased to test the speed. This test method showed the engine load response capability at different speeds. The speed and relative torque during the test cycle are presented in Figure 4. The parameter estimation of the TF, ARX, and ARMAX models was carried out by using the System Identification Toolbox (SIT) of Matlab. From the load response test, (T_c) and the engine speed n were fed as the input to the model. The orders of the ARX and ARMAX models and the poles and zeros of the TF were set manually, and the SIT used the commands `tf`, `arx`, and `armax` for parameter estimation. The SIT calculated R^2 values with the command `compare` to assess the prediction accuracy between (T_c) and the modeled torque.

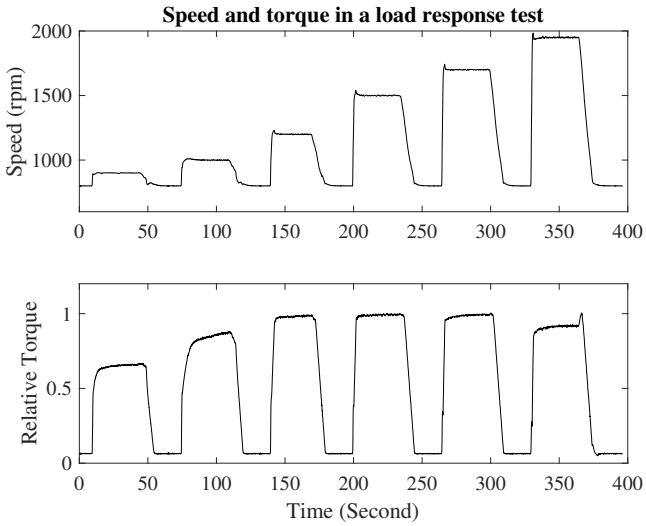

Figure 4. Engine speed and relative torque during the load response test.

Transfer function fitting and results

All the speed steps of the load response test were fitted into the TF separately. These steps are indicated by "ls" in the results in Table 2. The TFs with 2–3 poles and 2–3 zeros produced the highest R^2 results at different engine speeds. The percentage R^2 values, corresponding to each speed for different numbers of poles and zeros denoted by "p" and "z", are presented in Table 2. The lower R^2 values of the 1000 rpm fit results indicate a lower accuracy than in the other cases. Figure 5 shows that T_{Real} increased for a longer time during the load step, and that the shape of the torque response is different compared with the other speeds. The two highest-degree TFs (p3z2 and p3z3) at the speed of 1000 rpm produced higher R^2 values, and thus, a better fitting accuracy. However, these TFs caused oscillations in subsequent simulations. Hence, the TF with two poles and two zeros (p2z2) was chosen for the 1000 rpm case as the most suitable fit. The selected values are given in boldface in Table 2.

Table 2. R^2 values (logged as percentages) of the transfer function and real torque fittings at different speeds of the load response test data. The values of "p" and "z" are the numbers of poles and zeros. The bolded values are values that were chosen in the model comparison. The letter code "ls" refers to each load step in a particular engine speed. The speed ranges are presented in Table 3.

TF	p1z0	p1z1	p2z1	p2z2	p3z2	p3z3
ls900	93.49	93.49	93.85	**94.18**	93.84	93.84
ls1000	88.32	89.02	89.24	**89.39**	89.39	90.20
ls1200	93.02	93.02	93.75	94.05	**94.21**	77.99
ls1500	92.72	92.79	94.07	94.38	**94.57**	93.07
ls1700	92.40	92.61	93.99	94.32	**94.60**	94.42
ls1900	91.42	91.77	92.93	93.25	93.63	**93.68**

The model responses with these selected fitted parameter values are presented in Figure 5. The figure shows a comparison between the real engine torque command (T_c), the realized torque (T_{Real}), and the TF model-predicted torque (T_{tf}) during the test cycle. The fitted TF and its parameter values for each TF are presented in Appendix A in Table 10. The proposed method produced significantly different values of zero and pole parameters for each engine speed step. The best fitting accuracy was obtained with TFs of different orders at various speed steps. Interpolation of the TF parameters as a function of engine speed was not possible. Therefore, the chosen parameters were connected to the engine speed step by step as shown in Table 3.

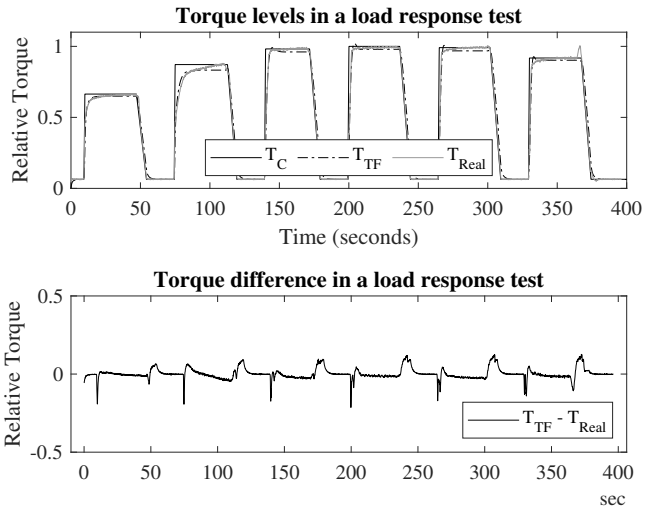

Figure 5. Transfer function (T_{TF}) method compared with torque command (T_C) and real engine torque (T_{Real}) during the load response test cycle.

Table 3. Engine speed ranges in which different transfer function and time series parameters were used step by step.

TF	Speed range (rpm)
ls900	$n < 950$ rpm
ls1000	950 rpm $\leq n <$ 1100 rpm
ls1200	1100 rpm $\leq n <$ 1350 rpm
ls1500	1350 rpm $\leq n <$ 1600 rpm
ls1700	1600 rpm $\leq n <$ 1800 rpm
ls1900	$n \leq$ 1800 rpm

Two transfer functions

The method of two first-order TFs (2TF) requires two parameters, one time constant (pole) for the increasing torque step s_g and the other for the decreasing step s_a. The principle of this method is presented in Figure 1. The time constant parameters s_g and s_a were fitted manually to produce the highest fitting results. The gas dynamics parameter s_g produces the highest R^2 value at 1.0 s, and the fuel actuator s_a was set at a value of 0.20 s. This combination produced an R^2 value of 99.38%. It should be noted that the parameter values were constant in the whole engine speed range contrary to the TF method; nevertheless, the R^2 values were significantly higher with the 2TF method than with the TF method. Hence, it was decided to keep the parameters constant over the engine speed range. Furthermore, no substantial cross correlation between these two parameters was detected. In Table 4, R^2 values at different parameter values are presented. In addition, the torque responses of the 2TF model are depicted in Figure 6.

Table 4. R^2 fitting values (in percent) between the 2TF method and real torque at different speeds of the load response test data. The bolded values were chosen for model comparison.

Gas dyn. delay (S_g)	R^2	Actuator dyn. (S_a)	R^2
0.75	99.28	0.05	99.36
0.80	99.32	0.10	99.37
0.85	99.34	0.15	99.38
0.90	99.36	0.20	**99.38**
0.95	99.37	0.25	99.37
1.00	**99.38**	0.30	99.37
1.05	99.37	0.35	99.36
1.10	99.36	0.40	99.34
1.15	99.35	0.45	99.32
1.20	99.33	0.50	99.30

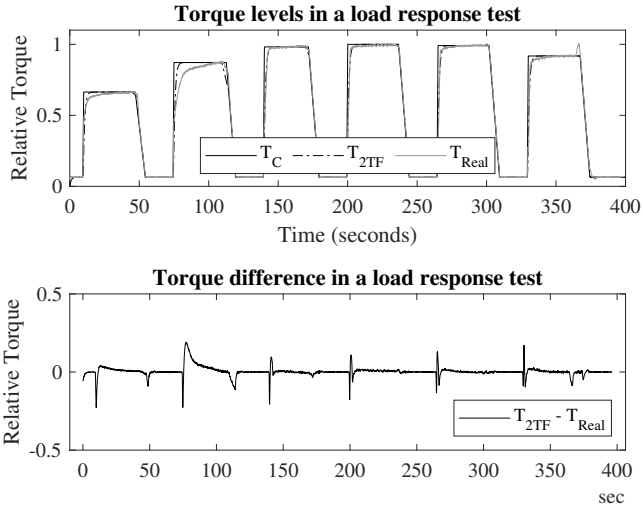

Figure 6. Two transfer functions (T_{2TF}) method compared with commanded torque (T_C) and real engine torque (T_{Real}) during the load response test cycle. The parameter values that produced the highest R^2 values were used.

Autoregressive time series

According to the TF method, the time series parameters were fitted separately at each speed step of the load response test by the SIT. It used the commands *delayest* and *arx* to perform model parameter fitting. The order of the time series refers to the number of time steps in the past data (the time shift operator q in Equations (1) and (2)). These orders were kept as low as possible.

The ARX model torque responses are shown in Figure 7, and the R^2 values are shown in Table 5. The best R^2 values of different load steps were in the range of 92.4–94.2%, excluding the 1000 rpm load steps, for which the best fitting result was 89.4%. The optimal time steps at each engine speed were in the range of ARX 211–333, and the parameter values in boldface were chosen for the ARX model.

The parameter estimation process of the ARMAX models was similar to the ARX procedure. The highest R^2 values in each speed were chosen, and the parameter values were connected to the engine speed step by step according to

Table 5. R^2 values (in percent) between the ARX time series and real torque at different speeds of the load response test data. The bolded values are values that were chosen for model comparison. The time series are classified by numbers. These numbers consist of the time steps of the parameters A and B and the delay parameter n_{k_i}. The ARX 110 was of the lowest order, and the ARX 333 was the most complex model. The letter code "ls" refers to each load step at a particular engine speed. The speed ranges are given in Table 3.

ARX	110	111	211	221	222
ls900	93.41	93.46	93.15	93.17	93.54
ls1000	88.59	89.29	87.59	89.16	**89.38**
ls1200	92.66	92.70	**92.86**	92.37	92.23
ls1500	91.84	92.02	**92.89**	92.03	92.19
ls1700	91.13	91.43	92.56	91.87	91.97
ls1900	89.89	90.27	92.20	91.64	92.02

ARX	322	332	333
ls900	93.65	93.95	**94.18**
ls1000	89.33	89.24	88.51
ls1200	92.11	91.88	91.41
ls1500	91.74	91.82	91.56
ls1700	92.07	92.69	**92.73**
ls1900	91.67	**92.37**	92.32

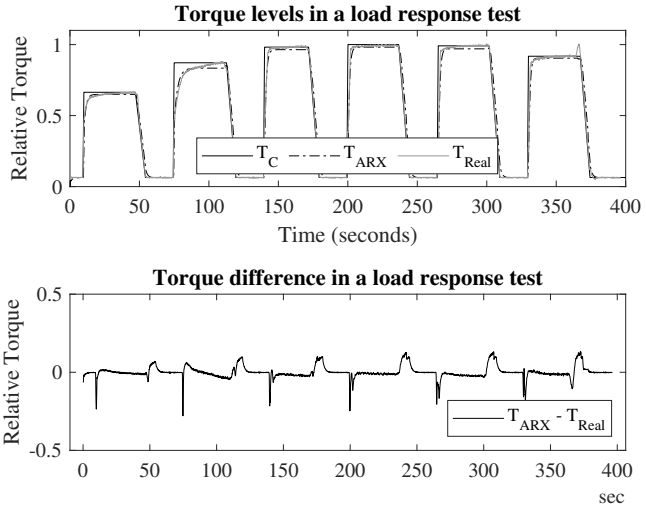

Figure 7. Torque produced by the fitted ARX model T_{ARX} compared with the commanded torque T_c and the real torque T_{Real} in the load response test.

Table 6. R^2 values (in percent) between the ARMAX time series and the real torque fittings at different speeds of the load response test data. The bolded values are the values that were chosen for model comparison. The time series are classified by numbers. They refer to the time steps of the parameters A, B, C, and the delay parameter n_{k_i}. The ARMAX 1100 was of the lowest order, and ARMAX 3222 was the most complex model. The letter code "ls" refers to each load step at a particular engine speed. The speed ranges are given in Table 3.

ARMAX	1100	1110	1111	2111	2211
ls900	93.42	93.27	93.28	93.38	93.25
ls1000	88.38	88.39	88.09	88.16	**88.87**
ls1200	92.26	92.91	**92.99**	92.86	92.56
ls1500	91.23	92.35	92.58	**92.62**	92.03
ls1700	90.35	91.78	92.16	**92.60**	91.91
ls1900	89.89	90.80	91.18	91.84	91.36

ARMAX	2221	2222	3222
ls900	93.61	93.86	**93.87**
ls1000	88.75	88.66	88.73
ls1200	92.44	92.23	91.97
ls1500	92.06	92.13	91.84
ls1700	91.73	91.87	91.60
ls1900	91.42	91.73	**92.74**

Table 3. In general, the R^2 values were at the same level between the ARX and the ARMAX models, and significant differences between the benefits of the model results were not noticed. In addition, the order of the time series did not offer benefits in the fitting accuracy; the best R^2 values were randomly at different orders in both the ARX and the ARMAX models. The ARMAX torque response graphs are shown in Figure 8, and the R^2 values are presented in Table 6. The estimated parameter values A, B of the ARX and A, B, C of the ARMAX models are given in Appendix A in Tables 11 and 12.

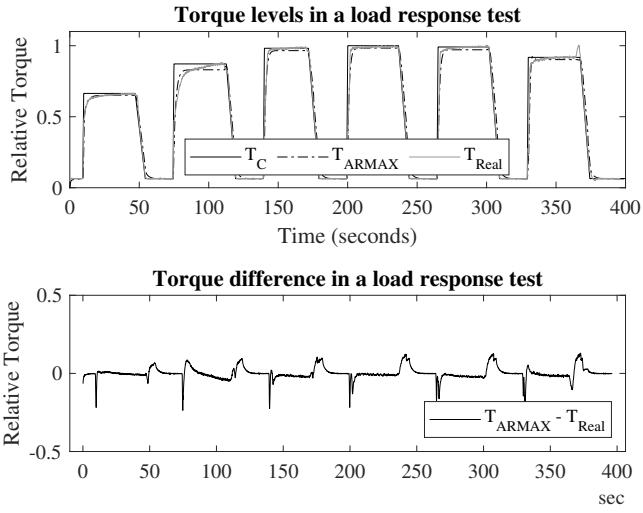

Figure 8. Torque produced by the fitted ARMAX model T_{ARMAX} compared with the commanded torque T_c and the real torque T_{Real} in the load response test.

DTL method

The parameter fitting of the DTL method includes estimation of one delay parameter S_d and two limitation parameters (a and b) according to Equation (3). The limitation parameter and the delay parameter were adjusted manually. Table 7 shows the R^2 values as a function of the parameter S_d. Figure 9 presents the DTL model torque responses compared in T_{real} in the load response test. It can be noticed that the R^2 values were at a significantly higher level when the DTL or 2TF models were used than in the case of the TF, ARX, or ARMAX method. The parameters a and b used in the parameter fitting are given in Appendix A and Table 13.

Validation of the selected models

Validation and comparison of different simulation methods were executed by using a Non-Road Transient Cycle (NRTC). The NRTC cycle is developed for emission testing purposes of off-road engines. It is 1238 s long, and the

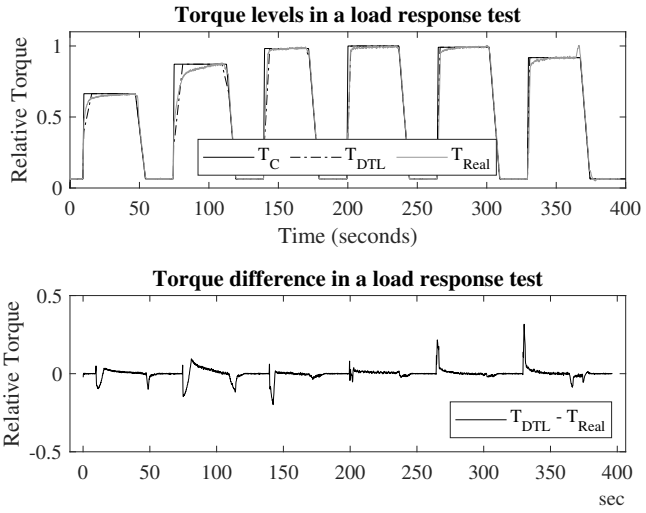

Figure 9. DTL model output torque compared with real engine data in the load response test.

Table 7. R^2 values (in percent) between the DTL method and real torque in the load response test data. The bolded value was chosen for the model comparison.

DTL delay parameter d (s)	R^2
0.05	99.35
0.10	**99.38**
0.15	99.37
0.20	99.35
0.25	99.32
0.30	99.27
0.35	99.21
0.40	99.14
0.45	99.05
0.50	98.96

engine speed and torque are varied to simulate real off-road engine duty cycles. The speed and torque profile of the tested engine during the NRTC cycle is shown in Figure 10. The commanded torque T_c and the engine speed profiles of the NRTC n were fed as input data into each fitted model. The simulated torques and the real torque T_{Real} of each model were compared. The comparisons were assessed by an R-squared regression analysis over the whole NRTC. The test engine was the same engine that is presented in Table 1.

A time slot from 330 to 360 s of the NRTC cycle was chosen to demonstrate the torque output of different simulation methods compared with the real engine output. This time period includes high torque ramps, and it is challenging for the engine dynamics. The regression results between T_{real} and each simulated torque were calculated over the entire NRTC cycle. The R^2 values are presented in Table 8. It can be concluded that the TF method (70.7%) and the ARX method (70.6%) had the lowest R^2 values, while the result of the ARMAX method was slightly higher, 71.4%. Figures 11 and 12 show that simulations in the increasing torque steps had a good correlation, whereas in the decreasing steps, an excess delay occurred in all three methods.

One reason for the poor correlation values in the decreasing torque steps can be the characteristics of the engine delay. The turbocharging delay only affects in the

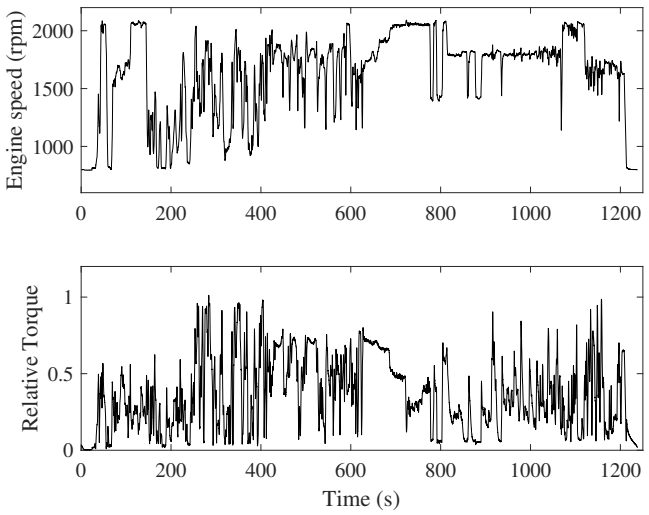

Figure 10. Speed and relative torque points of an NRTC cycle as a function of time.

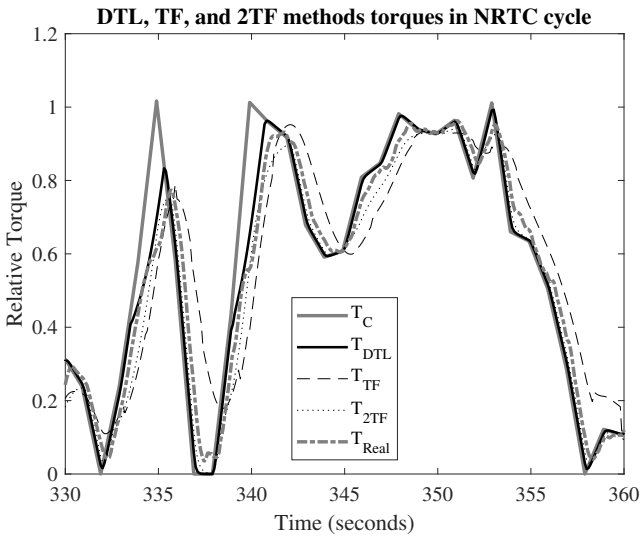

Figure 11. Comparison of the DTL, TF, and 2TF methods in the chosen period of an NRTC Cycle.

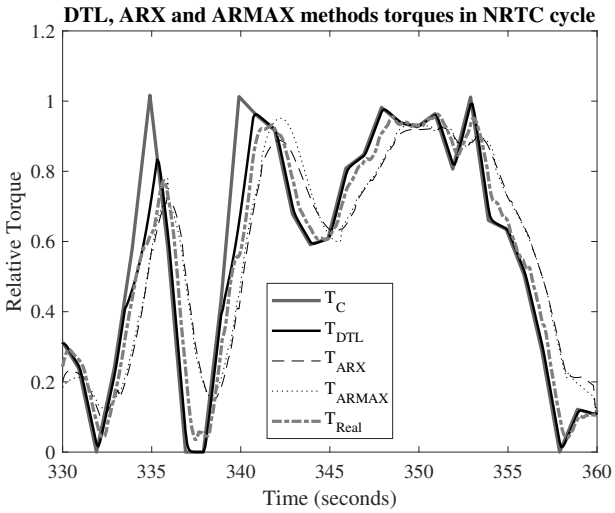

Figure 12. Comparison of the DTL, ARX, and ARMAX methods in the chosen period of an NRTC Cycle.

case of increasing torque steps, and for the decreasing torque steps, an additional slowness is present when similar TF and time series parameters were used in both steps. In the 2TF method, the fitting result was significantly higher, 84.3%. This is mainly due to the improvements at the decreasing steps, despite the fact that parallel TFs were the simplest ones. By increasing the complexity of the 2TF method (e.g., higher-order TFs, parameters as a function of speed, or even three parallel TFs) it is possible to make small improvements to the fittings; however, these improvements do not affect the prediction of the shape of the increasing torque steps, which is presented in the following.

Table 8. R^2 values (in percent) between the model output and the real engine torque in the entire NRTC Cycle with different simulation methods .

Simulation method	R^2 values over NRTC Cycle.
TF	70.7
ARX	70.6
ARMAX	71.4
2TF	84.3
DTL	91.1

Table 8 shows that the fitting accuracy can be improved by using the proposed DTL method; it produced the highest R^2 value, 91.1%, over the NRTC cycle. Figure 13 shows the increasing torque responses in the 1200 rpm load step in both the DTL and the 2TF method. It can be concluded that the DTL method even improves the correlation of the increasing torque steps, and it can simulate the realistic torque step form of a charged engine more accurately than the 2TF method.

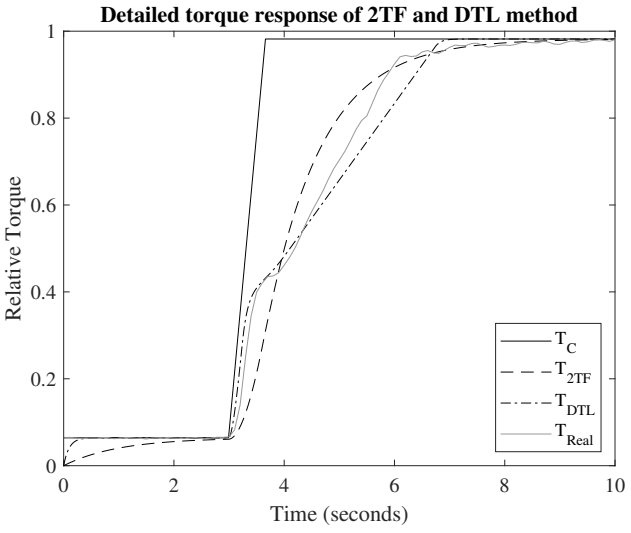

Figure 13. Detailed view of the increasing load steps of the DTL and 2TF methods at the 1200 rpm engine speed, compared with the real torque step.

DTL method applied to a constant torque test of a hybrid electric vehicle

To ensure the usability of the DTL method, it was applied to the engine data presented in (26). In the paper, a 5-cylinder turbocharged diesel engine was used in a series hybrid vehicle, where the engine was connected to an electric generator to produce electric power for the propulsion motor. Torque data of the combustion engine were collected from a constant torque power test. The generator produced constant torque for the engine, and it was accelerated from a constant speed to the maximum speed at full engine torque. These speed steps started from different static torques and speeds. In these tests, the instantaneous torque was the sum of the static and inertial torque of the rotational components. The static torque was produced by the electric generator, and the increasing speed in the engine–generator system caused inertial torque. The generator and shaft inertias were calculated from component masses and diameters assuming the parts as cylindrical components. Furthermore, an averaging of the measurement data was needed to filter the data oscillations. The inertia values of the components, data averaging, and sampling time are presented in Table 9.

Table 9. Constant torque test properties, inertia values, data filtering, and DTL model parameters for the hybrid electric vehicle under test.

	Value
Engine power (kW)	111
Engine torque (Nm)	290
Inertia of system (kgm^2)	0.734
Sample time (s)	0.04
Averaging of data	5-sample moving avg.
DTL Parameter T_d (Nm/s)	100
Time constant S_d (s)	0.3

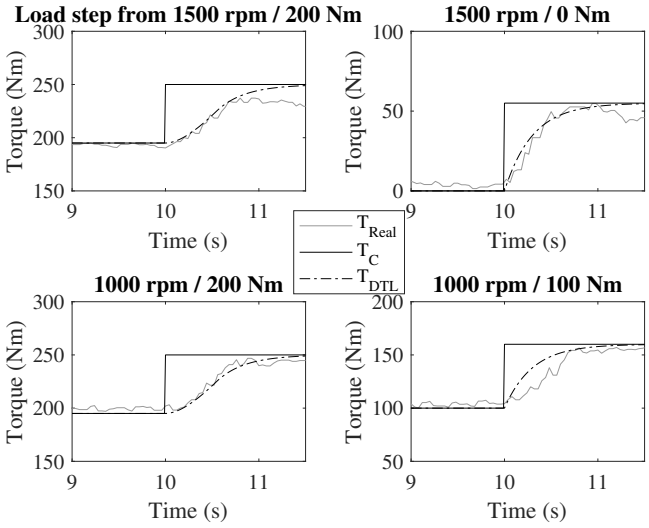

Figure 14. Engine load step data and modeled torque response of the DTL model in the constant torque tests for the hybrid electric vehicle under test.

Figure 14 shows four different torque steps of the engine and the responses simulated by the DTL method. A constant T_d parameter value was used, and thus, measured engine performance steps were not available. The values of T_d and S_d are given in Table 9. The main purpose of this study was to show that the DTL method can be used for simulation of different kinds of engines. It can be seen in Figure 14 that three of the four simulation results of the torque ramps correspond very well to the experiments. On the other hand, in the 1000 rpm / 100 Nm test point, the DTL method shows a faster response than the experiments. The reason for this may

be that the torque level was below the NAC level during the step, and the parameter S_d is only effective in this situation. Thus, this study shows that the DTL method is applicable even without the parameter estimation procedure.

Conclusion

This study showed a computationally efficient method to simulate the transient torque behavior of a turbocharged diesel engine. Extensive comparisons of different-order transfer functions (TF) and two statistical autoregressive time series models were performed by using real engine data. The increasing orders of the TFs or the autoregressive model time steps did not offer a significant improvement in accuracy. Using two different TFs, one for the increasing and the other for the decreasing torque steps, can significantly improve the prediction accuracy, even when the TFs used in the study were the simplest ones. The increasing torque step of the charged combustion engine consists of two parts; first, there is a fast response at low torques, and at higher torques, the delay increases as a result of the delay of the turbocharger. Time series or TF models cannot predict such a behavior accurately. The proposed Dynamic Torque Limiter (DTL) method can improve the prediction accuracy of the increasing torque step, because the method combines a time-based linear limitation parameter for the increasing steps and a computationally efficient first-order TF for the decreasing torque steps. One benefit of the DTL method is its straightforward calibration process, as there are only two or three parameters to calibrate. Because of the nonlinear phase behavior, it is not possible to calculate parameters from the output to input data backward. The modern off-road diesel engine data from an official emission test cycle NRTC were used to validate the torque simulation capability of each simulation method in heavily transient conditions. Simulated torque outputs and real engine torques over that cycle were assessed by R-squared regression analysis. These R^2 values over the NRTC were between 70.6% and 71.4% when the TF or autoregressive models were used. By using two different TFs for the increasing and decreasing steps separately (2TF), the regression can be improved to a value of 84.3%, and when using the DTL method, the regression was 91.1%. It can be concluded that the DTL method offers a computationally efficient simulation method for the transient simulation of a turbocharged combustion engine with a reasonably easy calibration procedure. In future studies, dynamic fuel consumption correlations for a static mapped engine should be determined.

References

References

[1] Tupitsina A, Montonen JH, Alho J et al. Simulation tool for dimensioning power train of hybrid working machine 2021; .

[2] Goswami G, Jaiswal S, Nutakor C et al. Co-simulation platform for simulating heavy mobile machinery with hydraulic actuators and various hybrid electric powertrains. *IEEE Access* 2022; 10: 105770–105785.

[3] Goswami G, Tupitsina A, Jaiswal S et al. Comparison of various hybrid electric powertrains for non-road mobile machinery using real-time multibody simulation. *IEEE Access* 2022; 10: 107631–107648.

[4] Baharudin E, Nokka J, Montonen H et al. Simulation environment for the real-time dynamic analysis of hybrid mobile machines. In *International Design Engineering Technical Conferences and Computers and Information in Engineering Conference*, volume 57168. American Society of Mechanical Engineers, p. V006T10A073.

[5] Mollenhauer K, Tschöke H and Johnson KG. *Handbook of diesel engines*, volume 1. Springer Berlin, 2010.

[6] Watson N and Janota M. *Turbocharging the internal combustion engine*. Macmillan International Higher Education, 1982.

[7] Feneley AJ, Pesiridis A and Andwari AM. Variable geometry turbocharger technologies for exhaust energy recovery and boosting-a review. *Renewable and sustainable energy reviews* 2017; 71: 959–975.

[8] Lee W, Schubert E, Li Y et al. Overview of electric turbocharger and supercharger for downsized internal combustion engines. *IEEE Transactions on Transportation Electrification* 2016; 3(1): 36–47.

[9] Winward E, Rutledge J, Carter J et al. Performance testing of an electrically assisted turbocharger on a heavy duty diesel engine. In *Proceedings of the 12th international conference on turbochargers and turbocharging*.

[10] Grönman A, Sallinen P, Honkatukia J et al. Design and experiments of two-stage intercooled electrically assisted turbocharger. *Energy Conversion and Management* 2016; 111: 115–124.

[11] ISO8528-5. *ISO 8528-5: reciprocating internal combustion engine driven alternating current generating sets-part 5: generating sets*. International Organisation for Standardization, 2018.

[12] Katrašnik T, Medica V and Trenc F. Analysis of the dynamic response improvement of a turbocharged diesel engine driven alternating current generating set. *Energy conversion and management* 2005; 46(18-19): 2838–2855.

[13] Rakopoulos C, Dimaratos A, Giakoumis E et al. Evaluation of the effect of engine, load and turbocharger parameters on transient emissions of diesel engine. *Energy Conversion and Management* 2009; 50(9): 2381–2393.

[14] Benajes J, Lujan J, Bermudez V et al. Modelling of turbocharged diesel engines in transient operation. part 1: insight into the relevant physical phenomena. *Proceedings of the Institution of Mechanical Engineers, Part D: Journal of Automobile Engineering* 2002; 216(5): 431–441.

[15] Luján JM, Climent H, Arnau FJ et al. Analysis of low-pressure exhaust gases recirculation transport and control in transient operation of automotive diesel engines. *Applied Thermal Engineering* 2018; 137: 184–192.

[16] Serrano J, Arnau F, Dolz V et al. Methodology for characterisation and simulation of turbocharged diesel engines combustion during transient operation. part 1: data acquisition and post-processing. *Applied Thermal Engineering* 2009; 29(1): 142–149.

[17] Hirata M, Hayashi T, Takahashi M et al. A nonlinear feedforward controller design taking account of dynamics of turbocharger and manifolds for diesel engine air-path system. *IFAC-PapersOnLine* 2019; 52(5): 341–346.

[18] Eriksson L. Modeling and control of turbocharged si and di engines. *Oil & Gas Science and Technology-Revue de l'IFP* 2007; 62(4): 523–538.

[19] Thomasson A and Eriksson L. Co-surge in bi-turbo engines: Measurements, analysis and control. *Control Engineering Practice* 2014; 32: 113–122.

[20] Sujesh G and Ramesh S. Modeling and control of diesel engines: A systematic review. *Alexandria Engineering Journal* 2018; 57(4): 4033–4048.

[21] Vong CM, Wong PK and Li YP. Prediction of automotive engine power and torque using least squares support vector machines and bayesian inference. *Engineering Applications of Artificial Intelligence* 2006; 19(3): 277–287.

[22] Hao D, Zhao C, Li YHG et al. Dynamic indicated torque estimation for turbocharged diesel engines based on back propagation neural network. *IFAC-PapersOnLine* 2018; 51(31): 720–725.

[23] Burke RD, Baumann W, Akehurst S et al. Dynamic modelling of diesel engine emissions using the parametric volterra series. *Proceedings of the Institution of Mechanical Engineers, Part D: Journal of Automobile Engineering* 2014; 228(2): 164–179.

[24] Zweiri Y, Whidborne J, Seneviratne L et al. A comparison of dynamic models of various complexity for diesel engines. *Mathematical and Computer Modelling of Dynamical Systems* 2002; 8(3): 273–289.

[25] Galindo J, Lujan J, Serrano J et al. Combustion simulation of turbocharger hsdi diesel engines during transient operation using neural networks. *Applied Thermal Engineering* 2005; 25(5-6): 877–898.

[26] Lindh T and Nevaranta N. Automatized method of moments to estimate process model of diesel engine dynamics. In *2020 25th IEEE International Conference on Emerging Technologies and Factory Automation (ETFA)*, volume 1. IEEE, pp. 1201–1204.

[27] Laurén M, Goswami G, Tupitsina A et al. General-purpose and scalable internal-combustion engine model for energy-efficiency studies. *Machines* 2021; 10(1): 26.

[28] Heywood JB. Combustion engine fundamentals. *1ª Edição Estados Unidos* 1988; 25: 1117–1128.

[29] Palma W. *Time series analysis*. John Wiley & Sons, 2016.

Acknowledgements

The authors would like to thank the engine and power train laboratory staff of the Turku University of Applied Sciences for the experimental research, and the AGCO Power, Finland for the collaboration concerning the experimental engine data, and also Mrs. Hanna Niemelä for checking the grammar.

Funding

The author(s) received no financial support for the research, authorship, and/or publication of this article.

Conflict of interest

The author(s) declared no potential conflicts of interest with respect to the research, authorship, and/or publication of this article.

APPENDIX A: Fitted parameters of transfer function, time series and DTL method parameters

Table 10. Fitted transfer functions' parameters

Load step	TF Parameters
ls900	$\frac{-0.3771s^2+2.222s+2.469}{s^2+4.716s+2.527}$
ls1000	$\frac{-0.2177s^2+2.561s+2.564}{s^2+6.709s+2.686}$
ls1200	$\frac{1.908s^2+1.692s+4.605}{s^3+5.386s^2+6.572s+4.695}$
ls1500	$\frac{1.986s^2+0.3304s+7.57}{s^3+5.009s^2+8.328s+7.714}$
ls1700	$\frac{2.021s^2-0.9832s+10.15}{s^3+4.56s^2+9.998s+10.37}$
ls1900	$\frac{-0.1961s^3+3.252s^2-4.971s+20.34}{s^3+5.07s^2+16.85s+20.67}$

Table 11. Fitted ARX parameters

Load step	Parameter A	Parameter B
ls900	$1-1.38z^{-1}+0.7154z^{-2}-0.2766z^{-3}$	$0.1314z^{-3}+0.2072z^{-4}-0.2814z^{-5}$
ls1000	$1-1.493z^{-1}+0.5111z^{-2}$	$0.2236z^{-2}-0.2058z^{-3}$
ls1200	$1-1.506z^{-1}+0.5423z^{-2}$	$0.03548z^{-1}$
ls1500	$1-1.6z^{-1}+0.629z^{-2}$	$0.02858z^{-1}$
ls1700	$1-1.548z^{-1}+0.5352z^{-2}+0.04331z^{-3}$	$0.1642z^{-3}-0.2484z^{-4}+0.1145z^{-5}$
ls1900	$1-1.709z^{-1}+0.8158z^{-2}-0.07749z^{-3}$	$0.162z^{-2}-0.2702z^{-3}+0.1375z^{-4}$

Table 12. Fitted ARMAX parameters

Load step	Parameter A	Parameter B	Parameter C
ls900	$1-1.75z^{-1}+0.8003z^{-2}-0.03993z^{-3}$	$0.1912z^{-2}-0.1809z^{-3}$	$1-0.02037z^{-1}-0.6563z^{-3}$
ls1000	$1-1.234z^{-1}+0.2764z^{-2}$	$0.1413z^{-1}-0.1006z^{-2}$	$1+0.6813z^{-1}$
ls1200	$1-0.9187z^{-1}$	$0.07989z^{-1}$	$1+0.888z^{-1}$
ls1500	$1-1.418z^{-1}+0.4596z^{-2}$	$0.04081z^{-1}$	$1+0.3716z^{-1}$
ls1700	$1-1.574z^{-1}+0.6044z^{-2}$	$0.02934z^{-1}$	$1-0.02716z^{-1}$
ls1900	$1-2.349z^{-1}+1.802z^{-2}-0.4465z^{-3}$	$0.01725z^{-2}-0.01002z^{-3}$	$1-0.6317z\ -1-0.2z\ -2$

Table 13. Utilized DTL method parameters a and b. These parameters pertain to Equation (3)

Parameter	Value
a	0.3357
b	-265.4